Comparative roles of upwelling and glacial iron sources in Ryder Bay, coastal western Antarctic Peninsula

Marine Chemistry 176 (2015) 21–33

Contents lists available at ScienceDirect

Marine Chemistry

journal homepage: www.elsevier.com/locate/marchem

Comparative roles of upwelling and glacial iron sources in Ryder Bay, coastal western Antarctic Peninsula

Amber L. Annett [a,*], Marta Skiba [b], Sian F. Henley [a], Hugh J. Venables [c], Michael P. Meredith [c], Peter J. Statham [b], Raja S. Ganeshram [a]

[a] School of GeoSciences, University of Edinburgh, Edinburgh, UK
[b] Ocean and Earth Science, University of Southampton, National Oceanography Centre, Southampton, UK
[c] British Antarctic Survey, Cambridge, UK

ARTICLE INFO

Article history:
Received 29 August 2014
Received in revised form 15 June 2015
Accepted 20 June 2015
Available online 27 June 2015

Keywords:
Iron
Aluminium
Iron budget
Glacial input
Upwelling
Ryder Bay

ABSTRACT

Iron (Fe) is an essential micronutrient for phytoplankton, and is scarce in many regions including the open Southern Ocean. The western Antarctic Peninsula (WAP), an important source region of Fe to the wider Southern Ocean, is also the fastest warming region of the Southern Hemisphere. The relative importance of glacial versus marine Fe sources is currently poorly constrained, hindering projections of how changing oceanic circulation, productivity, and glacial dynamics may affect the balance of Fe sources in this region.

Dissolved and total dissolvable Fe concentrations were measured throughout the summer bloom period at a coastal site on the WAP. Iron inputs to the surface mixed layer in early summer were strongly correlated with meteoric meltwater from glaciers and precipitation. A significant source of Fe from underlying waters was also identified, with dissolved Fe concentrations of up to 9.5 nM at 200 m depth. These two primary Fe sources act on different timescales, with glacial sources supplying Fe during the warm summer growing period, and deep water replenishing Fe over annual periods via deep winter mixing.

Iron supply from deep water is sufficient to meet biological demand relative to macronutrient supply, making Fe limitation unlikely in this area even without additional summer Fe inputs from glacial sources. Both glacial and deep-water Fe sources may increase with continued climate warming, potentially enhancing the role of the WAP as an Fe source to offshore waters.

1. Introduction

The Southern Ocean is the largest high-nutrient, low-chlorophyll (HNLC) region in the world, and holds the greatest inventory of unused nutrients in surface waters. Iron (Fe) is the primary factor limiting productivity in this region, as determined by several mesoscale, in-situ Fe-enrichment experiments (Boyd et al., 2007). In contrast, the sea–ice margins are not Fe-limited, as is evident from higher biological productivity, greater macronutrient utilisation and biological carbon dioxide (CO_2) drawdown (Carillo et al., 2004).

Several pathways supply Fe to the ocean, including estuarine and groundwater inputs, shelf/slope sediment resuspension, hydrothermal vent activity, glacial runoff, iceberg melt and atmospheric deposition (Boyd et al., 2012). In particular, the relative importance of glacial Fe sources remains poorly constrained (de Jong et al., 2012), with recent work indicating glacial Fe inputs are much greater than previously thought (Shaw et al., 2011; Hawkings et al., 2014). One of the most productive regions of the Southern Ocean, the western Antarctic Peninsula (WAP) shelf has been identified as a source region of Fe to the Atlantic sector (de Baar et al., 1995; Holeton et al., 2005; de Jong et al., 2012; Hatta et al., 2013). High Fe concentrations near shore result in a horizontal Fe gradient observed at distances up to 3500 km (de Jong et al., 2012).

Importantly, the WAP is undergoing dramatic changes in regional climate. It is currently the fastest warming region in the Southern Hemisphere (King, 1994; Vaughan et al., 2003). Changes have already been documented in ocean temperature and density structure (Meredith and King, 2005; Martinson et al., 2008), retreat of glaciers (Cook et al., 2005) and sea ice dynamics (Stammerjohn et al., 2008). All of these factors can potentially influence Fe inputs and cycling, raising questions concerning the consistency of the WAP as a source region for Fe inputs to the broader ocean. Recent studies (Boyd et al., 2012) suggest that the balance of Fe supply and use may change with global warming; in this context, the future evolution of the carbon pump in this setting is uncertain. Additionally, inputs from incursions of Circumpolar Deep Water (CDW; Moffat et al., 2009) and meltwater (Meredith et al., 2013) are balanced by export of shelf waters, some of which feed back into the Antarctic Circumpolar Current (ACC) in the

* Corresponding author at: School of GeoSciences, The Grant Institute, The King's Buildings, University of Edinburgh, James Hutton Road, Edinburgh EH9 3FE, UK.
E-mail address: amber.annett@ed.ac.uk (A.L. Annett).

http://dx.doi.org/10.1016/j.marchem.2015.06.017
0304-4203/

north via Bransfield and Gerlache Straits (Hofmann et al., 1996; Zhou et al., 2002), and where topography or cyclonic gyres direct the flow offshore (e.g., Beardsley et al., 2004; Klinck et al., 2004). Thus, changes in margin Fe sources have the potential to affect offshore waters.

In this study, we investigate sources of Fe by making measurements of dissolved Fe (dFe) concentrations and total dissolvable Fe (TDFe) concentrations during the austral summer of 2009–10 at a coastal site in Marguerite Bay on the WAP. Despite the importance of this region as a source of Fe, relatively few studies have measured Fe in the WAP region, and ship-based studies provide spatial coverage but limited temporal resolution. This is the first to monitor both dFe and TDFe throughout a bloom in the Antarctic sea-ice zone. Time-series and depth profile data are used to identify changes in Fe through time during a growing season, which we relate to inputs, water mass changes, and biological productivity. We also construct a detailed Fe budget for this site.

2. Methods

2.1. Study site and oceanographic setting

Ryder Bay is a shallow (maximum ~500 m) coastal embayment of Adelaide Island, open to Marguerite Bay to the south and bounded by the retreating Sheldon Glacier to the north (Fig. 1). Largely representative of Marguerite Bay (Clarke et al., 2008), Ryder Bay is subject to processes that influence physical and biogeochemical conditions throughout the coastal WAP region (e.g.: seasonal ice cover, glacial inputs). Further, it is the site of the Rothera Oceanographic and Biological Time Series (RaTS) programme conducted by the British Antarctic Survey at the nearby Rothera Research Station. Through this programme, water column conditions and biological activity have been monitored year-round in Ryder Bay since 1997 (Clarke et al., 2008). The accessibility of the RaTS site, long-term environmental dataset and proximity to a retreating glacier make Ryder Bay an ideal location for investigating the relative importance of glacial- and marine sediment-derived trace metal supply.

The Marguerite Bay region, along with the WAP, differs from many other Antarctic shelf regions in its proximity to the ACC, and the accelerating inputs of glacial meltwater from land. The oceanic source for WAP shelf waters is CDW, the warm, mid-level water mass of the ACC that arrives on the shelf in a less modified form than in other areas due to the absence of an Antarctic Slope Front (Klinck, 1998; Clarke et al., 2008; Meredith et al., 2008). CDW incursions are most pronounced near deep, glacially-carved canyons such as Marguerite Trough underlying Marguerite Bay (Moffat et al., 2008). Shelf circulation inshore of the ACC includes a southwestward flowing Antarctic Peninsula Coastal Current that is thought to enter Marguerite Bay at the northern end and exit near Alexander Island, although the detailed circulation within the bay remains uncertain (Moffat et al., 2009).

Water masses along the WAP shelf, including Marguerite Bay and Ryder Bay, have been described in detail (e.g., Clarke et al., 2008; Meredith et al., 2010). Briefly, warm (>1.0 °C), nutrient-rich CDW intrudes in relatively unmodified form onto the shelf (Martinson et al., 2008; Moffat et al., 2009), forming the dominant water mass at depth. Vertical mixing of CDW provides heat and macronutrients to the near-surface layers, with enhanced mixing occurring in coastal and shallow regions (Wallace et al., 2008). Above the CDW, heat loss and sea-ice

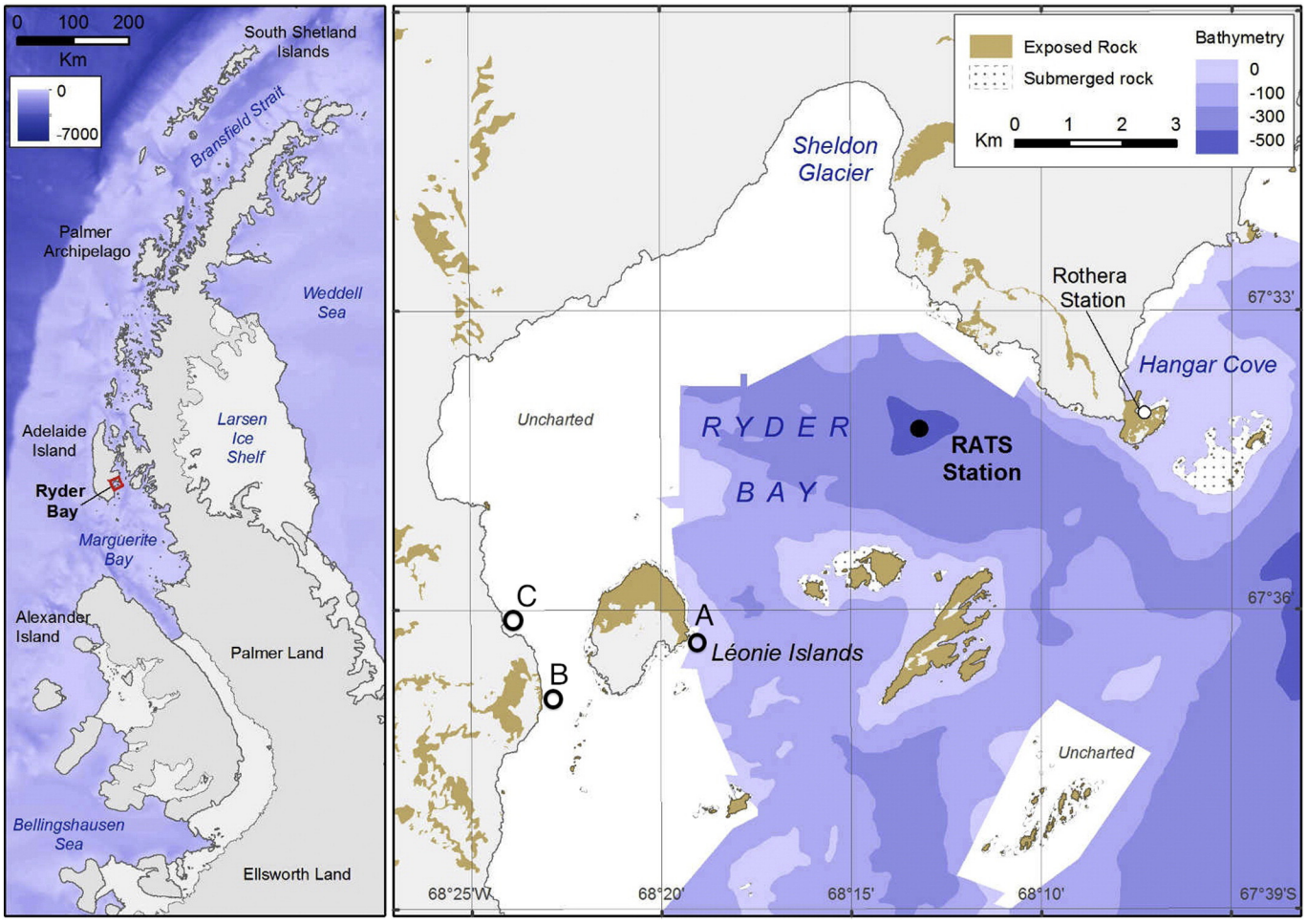

Fig. 1. Map of the western Antarctic Peninsula (left) and Ryder Bay (right), showing the RaTS sampling site and local bathymetry. Also shown are three additional sampling sites, two near exposed land (A, B) and one near the edge of a glacier (C).

formation in autumn and winter cools and adds salt to surface waters, resulting in a seasonally deep mixed layer of Winter Water (WW). In late winter, this water mass can extend downwards in a 50–150 m thick homogeneous layer, entraining CDW from below into the mixed layer (Meredith et al., 2004; Clarke et al., 2008). During spring and summer, the surface water is warmed by insolation and freshened by ice melt, leading to a stratified upper ocean with Antarctic Surface Water (AASW) overlying the remnant WW (Meredith et al., 2004).

Oxygen isotopes have been used to investigate freshwater inputs along the WAP (full sampling methodology, analysis and mass balance calculations are presented in Meredith et al., 2008, 2010, 2013). This work has identified meteoric (glacial and precipitation) water as the dominant source of freshwater to AASW during summer (Meredith et al., 2008, 2010, 2013). Meteoric freshwater typically accounts for 2–6% of the water at 15 m in Ryder Bay, compared with a maximum 2% contribution from sea-ice meltwater (Meredith et al., 2010). This range of meteoric and sea-ice meltwater contributions seen in Ryder Bay is similar to the variability seen throughout WAP region surface waters (2–6% meteoric water; −2 to 2% sea-ice meltwater (where negative values indicate net sea-ice formation); Meredith et al., 2013), indicating that the degree of glacial inputs at the RaTS site is relevant to surface waters at the regional WAP scale.

2.2. Sample collection

Samples for dFe and TDFe measurements were collected from Ryder Bay, Adelaide Island, Antarctica (Fig. 1) from December 2009 to March 2010. Samples were collected at the site of the RaTS programme, ~4 km from shore over a local maximum water depth of 520 m. Previous work at the RaTS Site has shown the primary water source to be open exchange with water masses from northern Marguerite Bay, although surface waters can be modified by glacial melt and local topography (Clarke et al., 2008; Meredith et al., 2010).

Samples were collected twice weekly from a depth of 15 m, to correspond with the suite of parameters analysed for the RaTS programme. This is the long-term average depth of the chlorophyll maximum and shows a very strong correlation to water column chlorophyll (Clarke et al., 2008). Deeper waters (50–200 m) were sampled approximately monthly, as weather and time allowed. Water samples were collected using a Teflon-coated 1.7 L Niskin-style sampler (Ocean Technical Equipment (OTE), Florida) that had been modified to have external springs and fluoroelastomer o-rings, and all stainless components of the bottle were coated with paint to prevent any corrosion. The original spigot was removed and replaced with a PTFE tap. The OTE bottle and PTFE tap were soaked for >24 h in 10% v/v HCl (Aristar grade) before each use, followed by thorough rinsing with deionised water (18.2 MΩ·cm, Millipore; hereafter "Milli-Q"). This is similar to the current GEOTRACES washing protocol (Cutter et al., 2010). The OTE bottle was deployed from a rigid inflatable boat, lowered on a Kevlar line and triggered with an acid-washed plastic messenger. On recovery of the OTE bottle, the water samples for TDFe were transferred via acid-cleaned (10% v/v HCl, >24 h) PTFE tubing into acid-cleaned and Milli-Q-rinsed 125 mL LDPE bottles (Nalgene; cleaning details below). This was done as quickly as possible to minimise exposure to air, after thorough rinsing of the tap, tubing and bottle (3 times) with sample. Samples for dFe were collected into 4 L acid-washed (10% v/v HCl, >24 h) HDPE bottles that had also been rinsed with seawater. Samples for dFe were then kept in the dark until processing in the lab, generally 2–3 h. The LDPE sample bottles were cleaned by soaking in 50% v/v HNO_3 (Reagent grade) for 1 week, 50% v/v HCl (Reagent grade) for 1 week, and were rinsed thoroughly with Milli-Q water. The bottles were then filled with Milli-Q and 1 mL L^{-1} UpA-grade concentrated HCl (Romil, UK), and stored until use (≥4 months). This cleaning protocol is similar to the GEOTRACES procedures published after this field work, and was chosen based on best practice at the time for trace metal sampling in coastal water systems.

On one occasion, surface samples were collected at locations near exposed land and a glacier terminus. These samples were collected by hand over the bow, just below the water surface. Bottles for both TDFe and dFe were rinsed three times with seawater and filled, using gloves and keeping the boat moving slowly into the surface current to avoid contamination from the boat. These were processed as for time-series samples.

2.3. Sample processing

Samples for TDFe were acidified with 1 mL L^{-1} of concentrated UpA-grade HCl and stored in the dark at room temperature for at least 10 months prior to analysis. Most studies consider the TDFe fraction to be that which is leached under acidic conditions (pH 1.8–2) over a period of at least 6 months (Sedwick et al., 1997; Ardelan et al., 2010; Gerringa et al., 2012). The total Fe measured should thus allow comparison between our values and other studies which have used ≥6 month leaching times, although values measured will depend on the concentration and nature of suspended particles.

Samples for dFe were filtered through a polycarbonate membrane filter (Isopore 0.2 μm, 47 mm, Millipore) in a polysulfone filter unit (Millipore). This filtered fraction will also have included some colloidal Fe, which is in the size range of 1–200 nm. All filtration equipment and filters were soaked in 10% v/v HCl (Aristar grade) at least overnight and thoroughly rinsed with Milli-Q prior to each use. The filtrate container and fresh 125 mL LDPE sample bottle were rinsed with filtrate three times before filling, then the dFe sample was acidified and stored as for TDFe samples. To minimise contamination, all laboratory manipulations were performed in a Class 100 laminar flow hood.

2.4. Determination of dissolved and total dissolvable iron concentrations

Dissolved Fe concentrations were measured using flow-injection analysis with 8-hydroxyquinoline (8-HQ) immobilised resin for pre-concentration and *N*,*N*-dimethyl-*p*-phenylenediamine di-hydrochloride (DPD, Sigma-Aldrich) (FIA–DPD–NTA) after Measures et al. (1995). This method is based on the catalytic oxidation of DPD by H_2O_2 in the presence of Fe to create a bright pink-coloured semi-quinone derivative. Dissolved Fe in the sample is pre-concentrated on an 8-HQ chelating resin before being eluted into the reagent stream: the products of the reaction can be monitored using a spectrophotometer at 514 nm. The signal detection in this study was based on measured voltage, a proxy to measure the signal for transmission which can be converted to absorbance. This gives a quantitative measure of the reaction, which is converted to concentration by comparison with absorbance values of standards of known concentration. LabVIEW 7.1 software was used for instrument control and data collection, and a separate LabVIEW 6.1 programme for data processing. For lower Fe concentrations (<10 nM), peak heights were used; for higher Fe concentrations (>10 nM), peak areas were used as these gave a more linear calibration.

Certified reference materials (CASS-5, NASS-6) were analysed to ensure accuracy of Fe measurements (Table 1). The blank was estimated by measuring peak heights for samples of Milli-Q (0.51 ± 0.25 nM). The detection limit, based on 3 times the precision of the blank, is estimated at 0.75 nM, ~4-fold lower than the lowest dFe reported here. All analyses were conducted at the National Oceanography Centre (NOC), Southampton, UK.

Table 1
Concentrations and results of certified reference materials from duplicate analyses. Standards used were Nearshore Seawater Reference Material for Trace Metals (CASS-5) and Seawater Reference Material for Trace Metals (NASS-6; both from NRC, Canada).

Reference material	Fe concentration	Measured
CASS-5	25.78 ± 1.97	24.81, 26.81
NASS-6	8.86 ± 0.82	8.66, 9.95

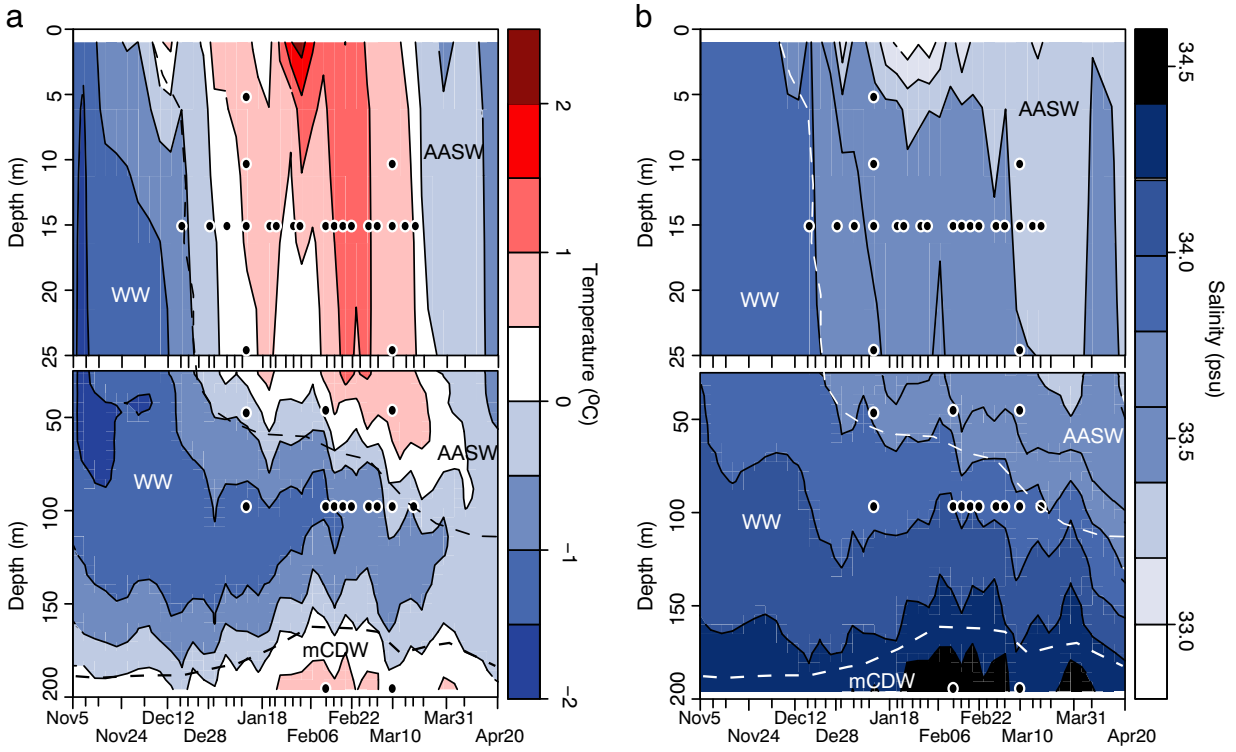

Fig. 2. Water column conditions at the sampling location (RaTS Site) with depth during the 2009–2010 summer season. Temperature (a) and salinity (b) are shown, and in each case the top 25 m of the water column is expanded in the top plot. Black dots denote sampling events. Dashed lines and text labels indicate the position and approximate boundaries between water masses (Antarctic Surface Water, AASW; Winter Water, WW; and modified Circumpolar Deep Water, mCDW).

Samples for TDFe were processed as for dFe, after gently decanting the solution into an acid-clean container to minimise transfer of any particulate material. There was no evidence for collection of particles on the resin column, as there were no high blanks, run periodically throughout the analysis, which could have resulted from Fe contamination from suspended material on the resin.

2.5. Determination of dissolved aluminium concentrations

Concentrations of dissolved and total dissolvable aluminium (dAl and TDAl, respectively) were determined following the Lumogallion method of Hydes and Liss (1976). Lumogallion (3-(2,4-dihydroxyphenylazo)-2-hydroxy-5-chlorobenzenesulphonic acid) reacts with Al to form a fluorescent complex. The fluorescence of samples can thus be compared to standards to determine dissolved Al. Measurements of Al were performed on the same samples collected for Fe analysis, and all analyses were performed at the NOC, Southampton, UK. A standard solution of Al was prepared from analytical grade aluminium potassium sulphate (1.758 g per 100 mL) to give a 1000 mg L^{-1} standard. This primary standard was diluted as needed to provide the standards used in the analyses. Samples for TDAl were treated as for TDFe, by decanting unfiltered samples that had been acidified to release a readily labile fraction of Al. As for Fe, the blank was estimated from measurements of Milli-Q (0.53 nM ± 0.21), and the detection limit (0.63 nM) was based on 3 times the precision of the blank. As no certified coastal reference materials exist for the determination of dissolved Al, measurement quality was assessed by good precision, and general agreement of data acquired here with published values for comparable marine settings.

3. Results

3.1. Physical and biological conditions

Over the study period, physical conditions in Ryder Bay (Fig. 2) indicate a typical summer trend of warming and freshening at the surface (top ~25 m). Whilst meteoric water is typically a greater component of fresh water input than sea-ice melt (Meredith et al., 2008, 2010, 2013), meteoric inputs rather than sea-ice melt are likely to be especially important for this study period, as sea-ice cover was low during the preceding winter.

Within the surface waters, chlorophyll *a* records show an initial increase in late November, coinciding with a reduction of the mixed layer depth (MLD). Following a deep mixing event on 15 December, concentrations then decline until a period of high-chlorophyll (>10 mg m^{-3}) lasting ~10 days in mid-February (Fig. 3). Peak chlorophyll concentrations (22 mg m^{-3}) occurred on 15 February, rapidly falling to <1 mg m^{-3} by 10 March. Trends in chlorophyll (as a proxy for biological production) are reflected in the concentrations of macronutrients nitrogen (N, from nitrate) and phosphorus (P; Fig. 3). These nutrients show a slight, gradual drawdown through the early part of the season, with a marked depletion to minimum values on 22 February.

3.2. Metal concentrations in surface waters

The concentration of dFe (3.5–9.4 nM; Fig. 3) was high in Ryder Bay compared with many areas of the ocean, but consistent with other coastal Antarctic studies (Table 2). Offshore surface water concentrations are generally very low (often <1 nM; Martin et al., 1990; de Baar et al., 1995; Bucciarelli et al., 2001), with significant enrichment in coastal areas. There is good agreement of dFe concentrations from this study and values reported for the Gerlache Strait (Martin et al., 1990),

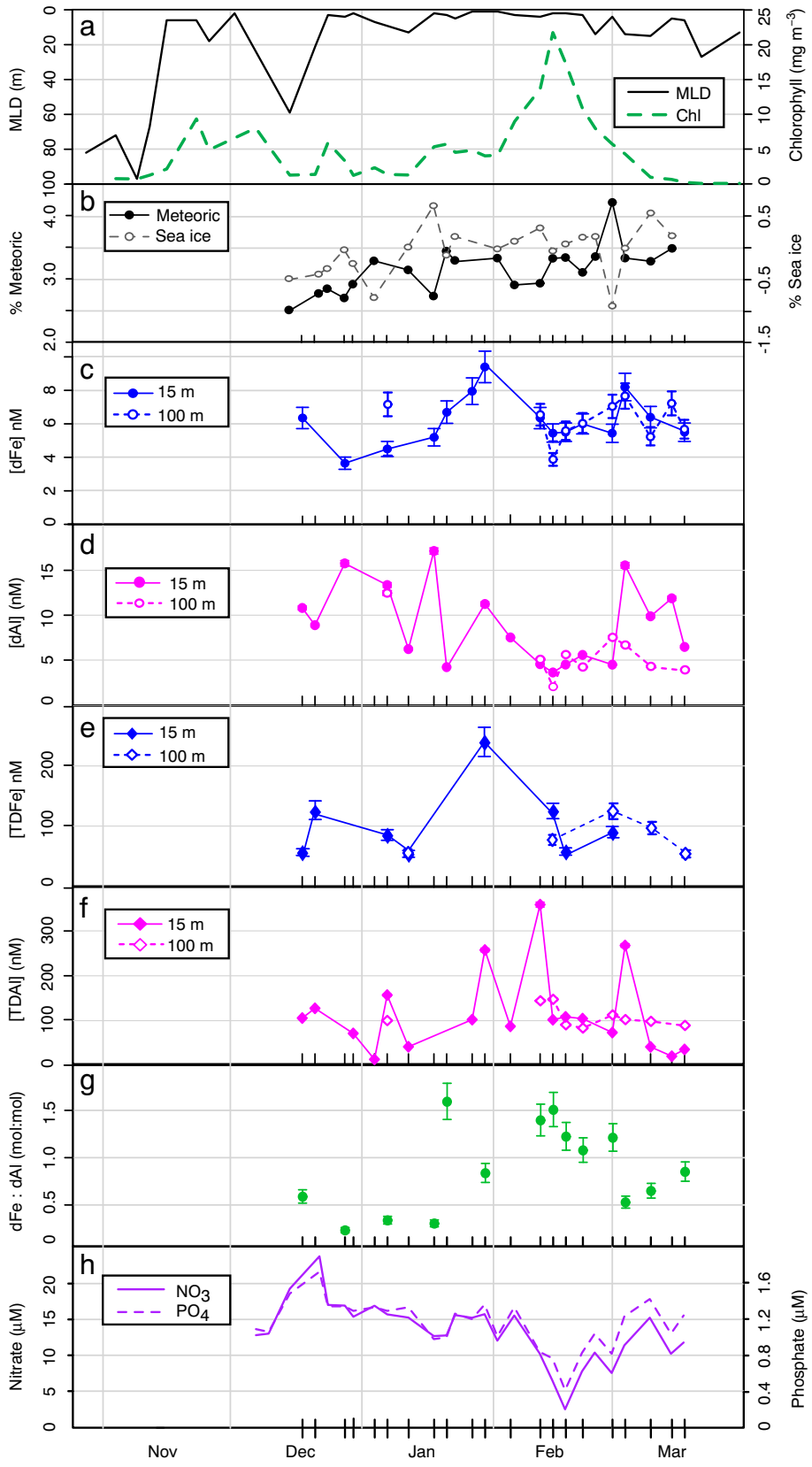

Fig. 3. (a) Mixed layer depth (MLD) at the RaTS site, and chlorophyll concentrations at 15 m. (b) Percent contributions of meteoric and sea-ice melt to the water column at 15 m. Data from Meredith et al., 2010. (c) Dissolved Fe concentrations at 15 and 100 m. (d) Dissolved Al concentrations at 15 and 100 m. (e) Total dissolvable Fe concentrations at 15 and 100 m. (f) Total dissolvable Al concentrations at 15 and 100 m. (g) Ratio of dFe:dAl at 15 m. (h) Nitrate (NO_3^-) and phosphate (PO_4^{3-}) concentrations at 15 m.

Table 2
Comparison of dissolved and total dissolvable Fe in Southern Ocean waters in the vicinity of the WAP. Where available, results are given as a range, or (mean ± standard deviation).

Study	Location	dFe (nM)	TDFe (nM)
Martin et al. (1990)	Drake Passage, surface	0.16	
	Gerlache Strait, surface	7.4	
Westerlund and Öhman (1991)	Weddell Sea	0.44–13	
de Baar et al. (1995)	Antarctic Circumpolar Current	0.4–1.3	
	Polar Front	1.5–2.5	
	Drake Passage	<0.25	
Löscher et al. (1997)	UCDW	0.6–1.1	0.9–2.3
Bucciarelli et al. (2001)	Kerguelen Islands	0.46–0.71	
	– offshore		
	– near shore (2 km), near surface	5.3–12.6	
	– near shore, near bottom	18.4–22.6	
Queroue et al. (2015)	– near shore, all depths	1.82–3.82	
Planquette et al. (2007, 2009)	Crozet Islands	0.086–2.48	0.15–13.2[a]
Hewes et al. (2008)	Weddell–Scotia confluence	0.35–3.05	
Ardelan et al. (2010)	Northern WAP	1–3	8–140
	– coastal		
	– offshore	0.1–3	
Hatta et al. (2013)	Northern WAP	3.23–4.69	
	– coastal		
	– offshore (ACC)	0.12–0.32	
Sañudo-Wilhelmy et al. (2002)	Weddell Sea, surface waters	(1.7 ± 0.46)	
	Northern WAP, coastal	4.5–31	
Weston et al. (2013)	Ryder Bay		9–50
This study	Ryder Bay	3.5–9.4	57–237
	– 15 m time-series		
	– all depths	3.3–9.7	56–237
Gerringa et al. (2012)	Amundsen Sea, mCDW	0.2–0.4	3–10
	– surface waters, <100 km from Pine Island Glacier	0.1–1.31	5–30
Planquette et al. (2013)	Amundsen Sea		15–122[b]
	– ice shelf, near surface		
	– ice shelf, ~250 m		9.3–29[b]

[a] Total metal concentrations of the large particulate (>53 μm) fraction.
[b] Total metal concentrations of the particulate (>0.45 μm) fraction.

northern WAP (Sañudo-Wilhelmy et al., 2002) and near the Kerguelen Islands (Bucciarelli et al., 2001).

Sampling was most frequent at 15 m, the long-term average depth of the chlorophyll maximum (Clarke et al., 2008). At this depth, dFe shows an initial decrease and a gradual increase throughout January to a maximum concentration of 9.4 nM (Fig. 3). During February, dFe decreases to ~6 nM, with a short-lived increase seen at the beginning of March.

Concentrations of dAl (3.5–17 nM; Fig. 3) show very good agreement with previous values for Ryder Bay at 15 m (2–27 nM; Hendry et al., 2010). At this depth, dAl initially displays high variability, with a period of sustained lower values (mean: 5 nM) coinciding with the period of low dFe. In the present study, a transient increase in dAl was observed along with the increase in dFe on 4 March.

Total dissolvable metals here refers to both the dissolved and particulate metal that is released by mild proton attack, and in the case of Fe should thus give an indication of labile or potentially bioavailable Fe. Total dissolvable Fe was present at much higher concentrations than dFe (50–230 nM; Fig. 3), and somewhat higher than previous values (9–50 nM; Weston et al., 2013), with the difference likely influenced by the much shorter leaching times (~1 month) used in the earlier study, and possible differences in suspended particle concentrations between sample sets. A distinct maximum occurred on 30 January, when a maximum was also seen in dFe. In keeping with variable dAl, TDAl exhibits a large range (16–360 nM; Fig. 3). Peaks in TDAl generally coincide with peaks in dAl, wherever data is available for both dAl and TDAl.

3.3. Metal concentrations with depth

Throughout the second half of the season, time-series samples were also collected from 100 m. Concentrations of dFe and TDFe were very similar to those at 15 m, whilst dAl, and TDAl showed less variability in deeper waters than at 15 m over the same period (Fig. 3c–f).

In addition to time-series samples, water was also collected from additional depths ~ monthly as time allowed. On three occasions, multiple samples (to 100 m or 200 m) were collected to investigate changes in dFe and TDFe concentrations with depth (Fig. 4a). A sub-surface minimum in dFe was present at 50 m (dFe = 3.8 ± 0.3 nM, n = 3), below which dFe increased to a maximum of 9.5 ± 0.3 nM (n = 2) at 200 m, the deepest water sampled. Slightly higher variability in dFe (6.2 ± 1.2 nM, n = 9) was seen at 100 m.

In contrast to higher Fe, Al displays relatively little evidence of enrichment (both dAl and TDAl) at depth (Fig. 4a). Data from 100 m show consistent dAl (~5 nM) and TDAl (~110 nM) through February and March, with one sample from early January having higher dAl (12.4 nM; Fig. 3d). As in time-series samples, shallow waters (<25 m)

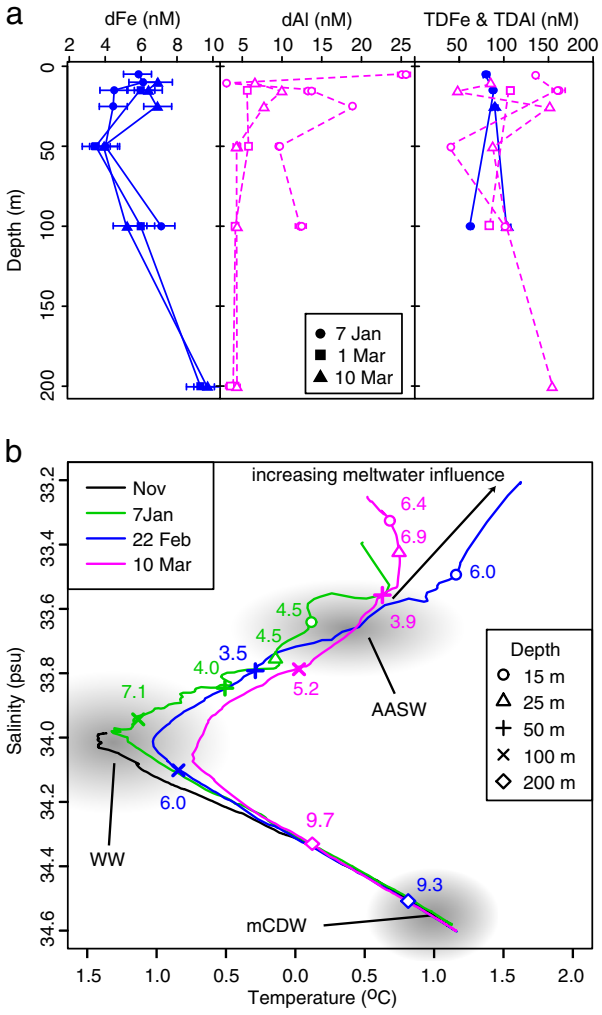

Fig. 4. (a) Dissolved Fe (left), dAl (middle) and total dissolvable Fe and Al (right) through the water column from three depth profile sampling events. Filled symbols are used for Fe, open symbols for Al. Error bars show the analytical precision or deviation between replicate measurements, whichever is larger. For Al, error bars are not shown where they are the same size as the symbol. (b) The association of dFe concentrations with water masses, where salinity is plotted versus temperature for four depth profiles from CTD data. Measurements of dFe (in nM) from discrete water samples are indicated by depth as shown in the legend. Shaded regions correspond to properties of mCDW (modified Circumpolar Deep Water), WW (Winter Water) and AASW (Antarctic Surface Water).

displayed considerable variability in both dAl and TDAl (Fig. 4), with the highest dAl measured at 5 m on 7 January.

4. Discussion

4.1. Sources of Fe to surface waters

Ryder Bay surface waters exhibit fluctuations in dFe over short time scales, reflecting a balance of Fe inputs and loss due to scavenging, biological use or mixing with lower-Fe water. Potential sources of Fe to surface waters include glacial melt (direct and via land run-off), sea-ice melt, sea water interaction with shallow sediments, and atmospheric inputs; sources from upwelling of deeper water are considered in Section 4.2.

Over the day-to-week scale of Fe enrichment seen here, atmospheric deposition in a low-dust environment is very unlikely to account for the significant surface signal seen in Ryder Bay. Iron can be released from shallow sediments, but this process is expected to be limited within the summer growing season as activities, mixing rates and water ages derived from radium isotopes all imply very low fluxes from the coast into central Ryder Bay (Annett et al., 2013).

A steady increase in dFe occurred from late December to 30 January (Fig. 3), when salinity decreases (Fig. 2), indicating an influx of low-salinity meltwater. Salinity averaged over the top 15 m of the water column (data not shown) indicates an even greater decrease in average salinity, thus the meltwater would have been present primarily above 15 m, consistent with a surface meltwater source. Whilst meltwater can potentially come from sea-ice, the low preceding winter sea-ice cover in the region and absence of sea-ice in Ryder Bay imply a meteoric source (glacial ice and snow) instead. Indeed, $\delta^{18}O$ data show a trend of increasing proportions of meteoric water at 15 m throughout the sampling period, from ~2.7% at the end of December to ~3.4% at the end of January (Fig. 3). The proportion of sea-ice melt also shows an overall trend of increase during this period, but with high sample-to-sample variability, including instances of reduced sea-ice contributions that correspond to increases in dFe, indicating that sea-ice melt is not the source of the Fe. Further, local observations indicate little or no sea-ice in Ryder Bay during the sampling period, thus the sea-ice signal in $\delta^{18}O$ at 15 m is likely due to lateral movement of AASW that has previously been subject to more or less sea-ice input, rather than reflecting recent sea-ice melt at the surface locally. In years of higher winter ice cover, sea-ice melt may affect dFe significantly, but this was not the case for the season presented here.

Further evidence for a glacial Fe source comes from three additional stations sampled to investigate variations in metal concentrations near a glacier terminus and exposed land (Fig. 5). The ratio of dFe:dAl for the glacier station (1.4) was much higher than for the two stations near exposed land (~0.3; Fig. 5), thus our data suggest that the glacier may be a greater source of Fe than of Al. Ratios of dFe:dAl at the RaTS site show a period of higher values during the middle of the summer season when glacial inputs are high (Fig. 3). In particular, the dFe:dAl ratio increases to 1.6 mol:mol on 21 January, when the contribution of meteoric water increases sharply to 3.4%, from 2.7% three days earlier, strongly supporting inputs from high Fe:Al glacial sources.

However, the late-season (4 March) increase in dFe does not show such a straightforward relationship with meltwater inputs, indicating that there are other sources of dFe variability in Ryder Bay surface waters. The increase in dFe at this time is likely due to mixing with deeper surface waters (below 15 m, but above the 50 m dFe minimum; see further discussion in Section 4.3). Overall, variations in dFe at 15 m reflect significant inputs from both meteoric meltwater and mixing with underlying waters (15–25 m), with no evidence for Fe input from sea-ice.

4.2. Deep water sources of Fe

Iron concentrations show a strong signal of enrichment with depth in Ryder Bay (9.5 ± 0.3 nM dFe at 200 m). This increase in dFe indicates a strong Fe source from the underlying sediment. No samples deeper than 200 m are available, but concentrations of Fe in CDW (<0.5 nM offshore; de Baar et al., 1995) the source for subsurface WAP waters, have been measured as 0.6–1.1 nM (Löscher et al., 1997) as it moves across the shelf and is modified (to mCDW). Thus, CDW must acquire Fe as it moves onto the shelf becoming mCDW, reflecting a

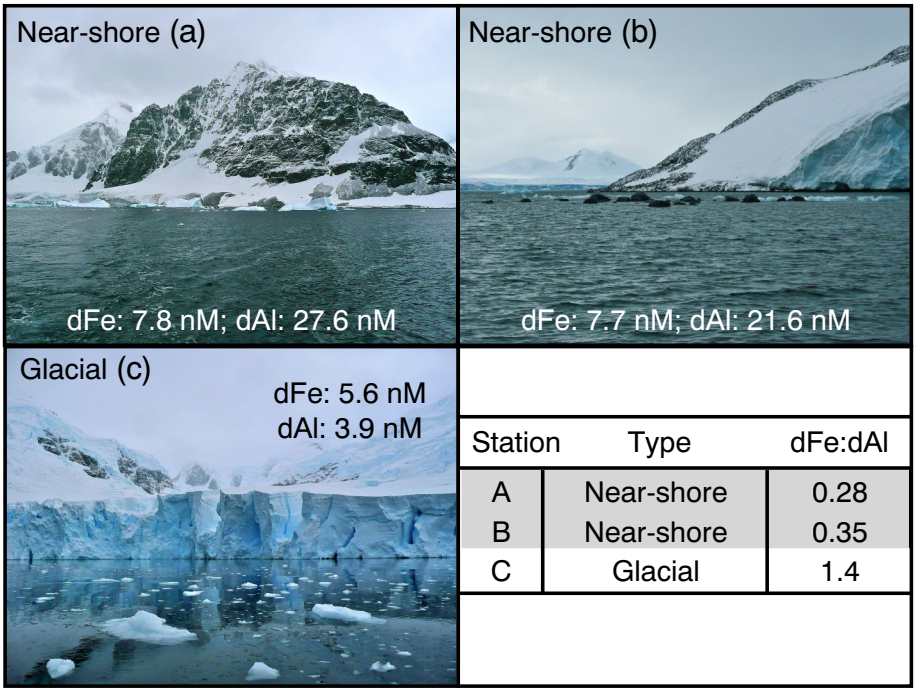

Station	Type	dFe:dAl
A	Near-shore	0.28
B	Near-shore	0.35
C	Glacial	1.4

Fig. 5. Surroundings and dissolved Fe and Al concentrations measured near exposed land (stations A, B) and the edge of a glacier (station C). Dissolved Fe:Al ratios (mol:mol) are given in the lower right panel. Locations are shown in Fig. 1.

strong sedimentary Fe source on the WAP shelf and/or slope, consistent with observations from other studies (de Jong et al., 2012; Gerringa et al., 2012; Ardelan et al., 2010; Dulaiova et al., 2009).

In comparison to Fe-limited Southern Ocean waters, the Fe concentrations measured at 200 m are high, but are in keeping with dFe measurements from locations with strong Fe sources. For example, Wu and Luther (1996) observed similar dFe (11–14 nM) and much higher TDFe (775–11,100 nM) in surface waters influenced by the Delaware Estuary; dFe throughout the shallow southern North Sea varies seasonally and over a range of <0.7–246 nM (Tappin et al., 1995). Near sediments on the Washington and Oregon shelves, hypoxic conditions lead to dFe concentrations up to 35 nM (Lohan and Bruland, 2008).

Iron supply from shelf sediments reflects the redox chemistry of Fe, and its speciation. In areas of high particulate organic carbon (POC) flux, microbial respiration can deplete oxygen, resulting in anoxic conditions within the sediments. If nitrate is also depleted, oxidation of POC proceeds via the reduction of Fe^{3+} and sulphate (SO_4^{2-}; Froelich et al., 1979). This microbially-mediated process produces Fe^{2+}, which is soluble in seawater. If there is a strong concentration gradient, and the redoxcline extends to the water column, this Fe^{2+} can diffuse out of sediment pore waters and into the overlying water.

The magnitude of sedimentary Fe release to overlying waters depends on several factors, including the solubility of such Fe^{2+} as it may be converted to the Fe^{3+} form when oxygen is present. Whilst organic ligands can help to retain Fe in solution, they are generally considered saturated and present in low concentrations in deeper waters (Johnson et al., 1997), and non-ligand bound Fe^{3+} above the solubility limit will rapidly form colloidal oxyhydroxides. Recent work indicates ~80% of dFe in sediment pore water is present as colloids, and thus likely stabilised in "dissolved" form (Homoky et al., 2011). Iron released from sediments by resuspension has been shown to adsorb rapidly onto particles, although this Fe is thought to be labile and may readily return to the dissolved phase (Homoky et al., 2012). These processes of organic complexation and colloid release/formation will lead to elevated near-bottom dFe that can then act as a source to shallower waters via upwelling, deep mixing or diffusion. Offshore Fe advection is already known to occur based on previous studies (Planquette et al., 2007; Dulaiova et al., 2009; Ardelan et al., 2010; Hatta et al., 2013), indicating that shelf sediments can be a significant source of dFe.

Upward flux of Fe in Ryder Bay during summer is likely to be minimal, as physical properties through the season show predominantly downward propagation due to the development of a low-density, meltwater-rich layer at the surface that depresses the other water masses (Fig. 2). The movement of these water masses (and development of a meltwater-rich surface layer) is reflected in dFe concentrations (Fig. 4b). Where modified CDW that intrudes onto the shelf reaches Ryder Bay, concentrations of dFe are ~9.5 nM (at 200 m depth). Samples from 100 m were near the centre of the WW layer, with dFe decreasing very slightly from 7.1 nM to 6.0 nM from 7 January to 22 February (potential temperatures of −1.1 and −0.84 °C, respectively). The lowest dFe concentration at this depth (5.2 nM) was from the March sample, in which water properties were strongly influenced by the overlying AASW (potential temperature 0.03 °C), consistent with a significant degree of mixing with lower-Fe AASW. Within the AASW layer (~50 m) dFe is ~4 nM. Above ~25 m, AASW mixes with meltwater, resulting in occasionally high dFe concentrations in these surface waters. Delivery and removal processes will be most variable in surface waters, due to fluctuations in meltwater flux and composition, productivity, particle load, and non-biological scavenging, in keeping with strong dFe and TDFe variations both in time and between depths (<25 m). In contrast, dFe appears more consistent in deeper water masses (WW, mCDW).

The association of dFe concentrations with Ryder Bay water masses (Fig. 4b), especially the dFe minimum in the AASW layer, has important implications for Fe supply in this location. The Fe-replete deep waters can act as a source of Fe to WW, and replenish Fe that is removed by biological uptake and physical removal processes. However, given the strong gradients restricting vertical mixing during summer this is unlikely to occur in the summer bloom period. Over winter, deep mixing and homogenisation of the upper water column will result in deep water supply of Fe being a significant source, redistributing Fe throughout the WW layer. Such enrichment from below is linked to very strong mixing during unstratified winter conditions (e.g., winter/spring storms), as even in March when stratification begins to break down, the MLD remains well above the depth of the dFe minimum. Thus the predominant Fe supply to surface waters during the summer growing season will be glacial Fe, rather than upwelling.

4.3. Decoupled sources of Fe and Al

Aluminium and Fe have several common sources, including atmospheric dust deposition, meteoric and sea-ice melt, terrestrial run-off, and lithogenic sources (either terrestrial or marine). Unlike Fe, Al is not redox reactive and thus redox processes in organic-rich marine sediments will enhance release of Fe relative to Al, although the higher solubility of Al which is not controlled by organic complexation may result in Al inputs being more long-lived. Due to the shared and unique sources of Fe and Al, trends in Al concentrations can be used to further constrain sources of Fe, as well as of Al itself.

We find a high degree of variability in dAl in Ryder Bay surface waters (15 m), reflecting significant and variable sources of Al in this region. Such fluctuations have been explained by a combination of upwelling and mixing with underlying waters enriched in Al due to sea-ice brine rejection (Hendry et al., 2010). However, in contrast to trends in dFe, the low and consistent dAl found at 100 and 200 m (Fig. 4) implies no deep Al source.

Previously measured Al in glacial ice and snow (72 and 98 nM respectively; Hendry et al., 2010) suggest that meteoric inputs are small in relation to water column concentrations. A glacial source is unlikely to explain fluctuations in dAl of greater absolute magnitude than the simultaneous changes in dFe, as the station sampled here near a marine-terminating glacier had a dFe:dAl ratio of >1 mol:mol (Fig. 5).

Despite elevated dAl concentrations, Hendry et al. (2010) concluded that sea-ice was not a significant source of Al to surface waters, due the low volume of sea-ice melt in Ryder Bay surface waters. To account for the dAl changes of January 18 and March 4, melting sea-ice would have had to contain 1.2–2 μM dAl, several orders of magnitude higher than literature values (20–40 nM, Hendry et al., 2010; 11 nM, Lannuzel et al., 2011). In agreement with Hendry et al. (2010), our results suggest a minor role for melting sea-ice in Al supply, especially considering the much lower sea-ice cover preceding the present study.

Atmospheric deposition can also be a source of Al. However, dust fluxes are very low in the Southern Ocean (~0.0075 mg m^{-2} d^{-1} around Adelaide Island; Wagener et al., 2008). Using a crustal Al fraction of 7.7% (Wedepohl, 1995) and solubility of 18% (Baker et al., 2006), this equates to a daily input of ~0.26 pmol L^{-1} if mixed evenly from the surface to our sampling depth of 15 m, negligible in comparison with dAl measured variability. Whilst we cannot rule out dust events from the runway at the Rothera Research Station as a potential Al source, such events are not expected to be significant at the RaTS site; Lohan et al. (2008) examined metal contamination in bivalves, with only the nearest station (within ~50 m of the runway) exhibiting any evidence of influence from aircraft operations relative to samples collected ≥100 m from the air strip.

The remaining potential mechanism is Al release from shallow sediments, due to diffusion or resuspension, which could then be advected from the margins to central Ryder Bay. The high dAl found at stations A and B (Fig. 5), both near exposed land and very shallow waters (<15 m water depth), support shallow sediments as a significant source of Al. In contrast to the respiration-driven redox release of Fe from deeper sediments, a shallow sediment source may release more

Al from lithogenic material owing to more intense physical disturbance (e.g., from tides, waves and iceberg scour) and the Fe:Al crustal ratio (~0.2; Wedepohl, 1995). This release may be due to dissolution and desorption for dissolved phases, but also include release of colloidal and particulate metals, and the smaller colloidal Al would be included in the dissolved samples measured here. Physical processes in shallow sediments would also release Fe, and a dFe:dAl ratio of 0.3 at these stations is in keeping with a combination of metal release predominantly from lithogenic material (~0.2 Fe:Al) but with some contribution of Fe from redox-driven diagenesis. Further, the smaller dFe increase (2.8 nM) at the RaTS site accompanying the 11 nM increase in dAl is consistent with mixing with underlying water that is influenced by shallow sediment sources with low dFe:dAl.

The ratios of dFe:dAl at 15 m at the RaTS site (Fig. 3) can be divided into three periods. Early in the season, dissolved ratios in surface waters are similar to those measured at stations A and B, which are likely to have a strong sediment influence. Mid-season, when productivity and meteoric water contributions are higher, ratios increase to values very similar to that measured near the glacier. We therefore infer that during the early season, Al inputs derive primarily from shallow sediment sources mixed into WW by lateral advection and deep winter mixing. As melting proceeds over summer, glacial (lower-Al) sources dominate the inputs to surface waters, with higher-Al waters present deeper in the water column, below the glacial melt-dominated layer. This high-Al subsurface water does not then reflect a subsurface source of Al, but rather that high-Al surface water is displaced downwards by surface inputs of lower salinity meltwater during summer. This mechanism is consistent with a signal of very low coastal sediment inputs at 10 m during mid-summer inferred from radium activities in mid-Ryder Bay (Annett et al., 2013), and significant glacial Fe flux during the middle of the season.

Late in the season when mixing increases, intermediate dissolved metal ratios reflect an autumnal mixing of meteoric-derived surface waters and sediment-influenced sub-surface waters. This subsurface water would likely also be a source of Fe, for instance when dFe increases along with dAl on 4 March. At this time the dFe:dAl ratio changes from 1.1 to 0.5, suggesting a transition from glacial to non-glacial sources of metals. A shallow sediment source for subsurface dAl does not necessitate the source of Al from brine rejection and cascades hypothesised by Hendry et al. (2010). Runoff from land and tidal/wave action can explain sediment supply, resuspension and Al release, although sea-ice related processes may act to enhance Al enrichment from shallow sediments during winter.

The TDAl concentrations are much higher than dAl, and will include dAl, larger (>0.2 μm) colloidal Al, as well as simple adsorbed forms, Al co-released with Fe oxyhydroxides, and other weathering products on the surface of particles. Al can also be incorporated into biogenic particles via uptake and incorporation into opal. An evaluation of how reactive these forms of Al may be is beyond the scope of this study, but the TDAl data indicate a significant pool of environmentally available Al. The greater range of concentrations in surface waters is consistent with the greatest variations in input and removal processes occurring in shallow waters (time-series data at 15 versus 100 m, Fig. 3). More uniform concentrations were observed at 100 m and no enrichment in dAl was observed at 200 m (Fig. 4), pointing to a lack of Al source at depth, in contrast to Fe. The enrichment seen in TDAl at 200 m (Fig. 4) may reflect an increase in scavenging as particles sink, as observed in higher core-top Al/Si ratios beneath Ryder Bay (Hendry et al., 2010).

4.4. Biological Fe use and potential for Fe limitation

As Fe is an essential micronutrient, biological processes influence its distribution via uptake and remineralisation. Due to the high biological requirement for Fe relative to its scarcity in seawater, Fe is a metal with one of the strongest relationships with productivity. Thus, dFe concentrations in Ryder Bay are likely influenced by phytoplankton dynamics.

Chlorophyll concentrations in Ryder Bay, ~5 mg m^{-3} during the second half of January, show a steep increase beginning 2 February and peak at >20 mg m^{-3} on 15 February (Fig. 3). This chlorophyll peak was dominated by diatoms (Annett, 2013). At the same time, dFe fell by ~4 nM from the seasonal maximum on 30 January, to 5.5 nM, consistent with biological uptake of Fe with additional removal by inorganic scavenging during this period.

During such a drawdown event, changes in Fe and nutrient concentrations should reflect the relative biological utilisation of these elements. From the inverse of the slopes in Fig. 6, Fe to nutrient use ratios are 360 μmol:mol, and 370 μmol:mol for dFe:N and dFe:Si, and 5.1 mmol:mol dFe:P, respectively. Particulate elemental ratios measured at the RaTS site for C:N and C:Si (6.4 and 11.7, respectively; Henley, 2012) and the Redfield ratio for C:P (106:1) were used to express the above ratios in terms of C (dFe:C). The resulting Fe:C estimates of 53, 32 and 48 μmol:mol (from N, Si and P, respectively) are very similar to the ~40 μmol Fe:mol C estimated by Twining et al. (2004) for Fe-replete phytoplankton.

Iron limitation is a significant constraint on productivity in many of the world's oceans (Boyd et al., 2012). In general, coastal areas are considered unlikely to exhibit Fe limitation, due to the proximity of land-derived sources, and upwelling of Fe-rich deep waters. To our knowledge, this is the first study of dFe from the WAP region that spans the full period of peak chlorophyll, and indicates that Fe does

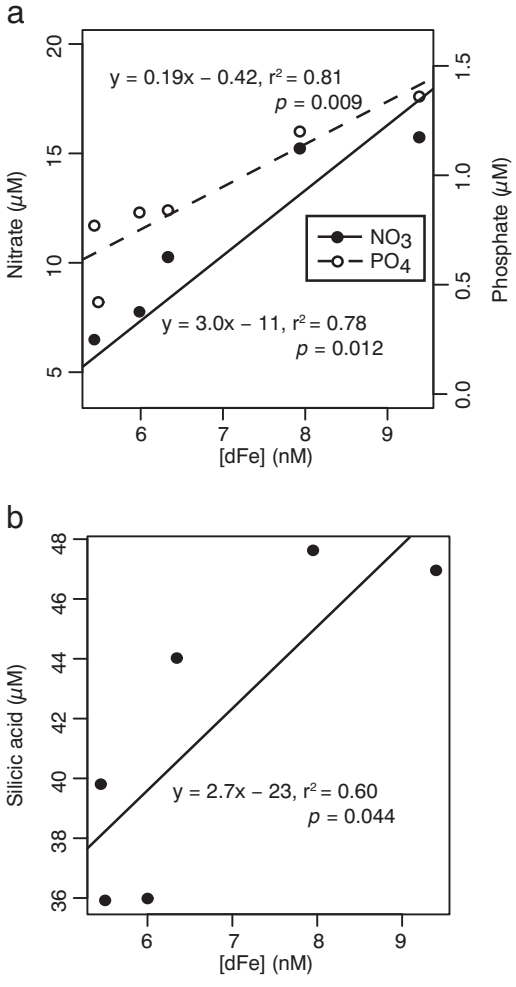

Fig. 6. Macronutrients (N and P: a; Si: b) versus dissolved Fe in 15 m water samples. Only the period of 30 Jan to 18 Feb was used, as biological activity dominated the Fe signal during this period whereas non-biological lithogenic inputs had strong effects on dFe outside of this time period.

not limit production even during peak productivity, consistent with TDFe data in this area (Weston et al., 2013).

However, high biological demand has been demonstrated to cause sporadic Fe-limitation even in coastal waters (Hutchins et al., 1998), and Ryder Bay and the WAP as a whole are areas of intense summer productivity (Clarke et al., 2008). The growing season sampled here displayed relatively low chlorophyll compared to other years at the same site (see Clarke et al., 2008; Venables et al., 2013), thus biological Fe use could potentially deplete the available Fe during more intense bloom periods. Ultimately, the ratio of macronutrients supplied to the surface mixed layer compared to the supply of Fe determines which (micro)nutrient will be depleted first, and therefore whether Fe has the potential to limit productivity in Ryder Bay.

Values for Fe-replete phytoplankton in the field are ~40 μmol Fe:mol C (Twining et al., 2004), and culture work indicates that diatoms are unlikely to suffer Fe stress at ratios above 10 μmol Fe:mol C (Sunda and Huntsman, 1995; Maldonado and Price, 1996). A recent review highlighted even lower ratios from non-Fe limited cultures, bulk particle analysis and dissolved nutrient profiles (4.7–56 μmol Fe:mol C; Twining and Baines, 2013). Macronutrient and dFe concentrations from deep water (100 m) in Ryder Bay indicate that supply of nutrients from depth will have ratios of 200–340 μmol/mol Fe:N and 2.5–-4 mmol/mol Fe:P (equivalent to 30–52 and 24–38 μmol Fe:mol C, respectively; Table 3). Thus the Fe supply from Ryder Bay deep water is adequate or high relative to N, although Fe:P supply is slightly lower than the demand for Fe-replete cells. However, both Fe:N and Fe:P are at least 2-fold higher than the ratios for Fe-stressed cells, indicating that the supply of Fe from below is sufficient to prevent Fe-limitation in Ryder Bay.

The change in nutrient concentration with depth also reflects biological uptake of nutrients, as well as abiotic scavenging processes. The ratios of this change in nutrient concentration at the RaTS site (determined from the slope of nutrients versus depth: 50–200 m for Fe; 15–100 m for N, P; macronutrients from Henley, 2012) are 140–460 (mean = 280) μmol:mol Fe:N, and 2.1–5.0 (mean = 3.8) mmol:mol Fe:P, consistent with nutrient use ratios from the surface water drawdown event, and in very good agreement with ratios for Fe-replete phytoplankton. Whilst a portion of this will come from scavenging rather than biological uptake, even these lowest ratios are still well above those for Fe-stressed phytoplankton (0.5–1 mmol:mol Fe:P in the North Atlantic, compared to 0.2 mmol:mol for Fe-limited regions of the Southern Ocean; Twining and Baines, 2013).

Different rates of micro- and macro-nutrient cycling have the potential to result in Fe limitation if macronutrients were recycled more efficiently than Fe, which could become progressively depleted relative to N or P supply. However, Twining et al. (2014) observed faster cycling of trace metals relative to macronutrients, making recycling likely to enhance dissolved Fe:N and Fe:P ratios. Thus dissolved nutrient profiles also indicate that Fe-limitation is unlikely in Ryder Bay, and that the deep water source of Fe is adequate to support complete drawdown of upwelled macronutrients.

Table 3
Deep water (100 m) nutrient and Fe concentrations and ratios for dates where all three elements were measured.

Date	Fe (nM)	NO_3^- (μM)	PO_4^{3-} (μM)	Fe:N (μmol/mol)	Fe:P (mmol/mol)
Jan 7	7.1	24.4	1.86	287	3.82
Feb 12	6.5	19.23	1.62	338	4.01
Feb 22	6.0	30.11	2.4	199	2.50
Mar 10	5.15	22.58	2.05	228	2.51
Range				200–340	2.5–4
Fe:C[a]				30–52	24–38

[a] Converted to Fe:C ratio based on the Redfield ratio (106:16:1 for C:N:P).

4.5. Iron budget

Glacial sources have already been shown to contribute significantly to Southern Ocean Fe supply, thus it is not surprising that they are also highly significant in Ryder Bay. The contribution of meteoric water to the water column can be calculated based on salinity and $\delta^{18}O$ data (Meredith et al., 2008). The maximum extra meteoric water contribution at 15 m for the summer of 2009–10 is 2.6% (=4.2% in March 2010 minus 1.6% in October 2009; Meredith et al., 2013). Assuming this meltwater is evenly distributed within the top 15 m and using published measurements of (dFe) in glacial ice (5–50 nM dFe; Raiswell et al., 2008) gives a seasonal input of 1.9–19.5 μmol Fe m^{-2}. If melt is constant during the 130 day season, this equates to an average daily flux of 15–150 nmol Fe m^{-2} d^{-1} to the top 15 m of Ryder Bay. There is more uncertainty around TDFe content in glacial ice (9–86 μM, excluding an estimated 90% that will sink out as particulates; de Baar and de Jong, 2001; Raiswell et al., 2006), giving an estimated flux of 27–250 μmol Fe m^{-2} d^{-1} for total particle-reactive Fe. As melt will likely not be uniform throughout the season, daily input may vary considerably beyond these range estimates.

Further consideration reveals that this estimate of glacial Fe inputs is almost certainly too low, i.e., it is a robust lower limit. First, it assumes that the amount of meteoric water in surface waters is constant with depth, whereas the contribution of fresh meteoric water at the surface will be greater than at 15 m (see salinity in Fig. 2). Second, this method does not account for glacially sourced meteoric water with elevated Fe concentrations, such as from basal ice and runoff. Such "dirty" basal ice is frequently seen in Ryder Bay and would be expected to carry considerably more Fe due to the greater terrigenous material content. Basal ice estimates from the Northern Hemisphere indicate a sediment load ~80–400 times greater than "clean" ice (Raiswell et al., 2006, and references therein). Glacial runoff has been sampled in the Dry Valleys, Antarctica, with dFe concentrations of 1.1–3450 μM (Sheppard et al., 1997; Green et al., 2005; Mikucki et al., 2009). Thus if even a small proportion of the meteoric water is derived from basal ice or runoff, the estimate of glacial Fe input would increase significantly.

Finally, Fe may be supplied by methods associated with the presence of the glacier, but not strictly sourced from glacial melt. For example, resuspension of sediments in sea-water beneath the glacier or terrestrial sediment in sub-glacial flow can contribute to very high dFe and colloidal nanoparticle Fe concentrations (35 nM and >1000 nM, respectively; Hawkings et al., 2014), but are not included here. These factors (higher glacial proportions above 15 m, basal ice and runoff, and sub-glacial processes) indicate actual glacial Fe input will be higher than the estimate presented here. However, the magnitude of the difference from the true level of glacial inputs is partially offset by the inclusion of precipitation in meteoric water, and whilst precipitation is likely to be low compared to the glacial component, we cannot assume that it is negligible.

Whilst this analysis focuses primarily on dFe fluxes, our results indicate that glacial processes deliver a much greater particulate component (92 ± 52 nM, ~90% of TDFe), consistent with earlier studies (Raiswell et al., 2006; Statham et al., 2008; Raiswell, 2011; Gerringa et al., 2012). Much of this particulate material will sink out of the surface due to vertical settling (Boyd et al., 2012), but in the sediments this fraction may be subject to reduction to Fe^{2+} and subsequent dissolution into overlying waters. Even before reaching the sediments, particulate Fe may be available for phytoplankton use (Planquette et al., 2011). Although the proportion of available Fe and rate of release are still areas of active research, recent work by Thuroczy et al. (2012) suggests that release of glacial Fe and subsequent productivity results in undersaturation of organic ligands, which will favour the solubilisation of glacial Fe and enhance the proportion available to phytoplankton. In addition to a potentially bioavailable Fe source, particles also represent an important mechanism by which Fe can bypass biological utilisation in the surface mixed layers (Homoky et al., 2012; Planquette et al., 2013), and transport of particulate Fe

may be significant in many regions (Frew et al., 2006; Lam et al., 2006; Planquette et al., 2009, 2011).

Whilst glacial inputs are suggested to be both spatially and temporally variable, our estimate indicates that Fe inputs from surrounding glaciers are very large. However, the magnitude of supply must be considered relative to the demand for Fe. Seasonal budgets of Si demand associated with new production have been estimated from Si isotopic measurements, concentrations, and physical water column conditions (Annett, 2013). Using the biological Fe:Si ratios determined above, the Si demand can be converted to annual requirement of Fe for new production. Although this is based on Fe:Si ratios and thus only reflects diatom production, phytoplankton biomass at the RaTS site is diatom-dominated (Clarke et al., 2008; Annett et al., 2010). The estimate of Fe requirement for 2009 is 130–260 μmol Fe m^{-2} y^{-1} in 2009–2010, and ~400 μmol Fe m^{-2} for a high-chlorophyll year. Further, as the Fe:Si ratios calculated from drawdown will also include scavenging of Fe, the true biological Fe requirement will be less than these estimates suggest.

The dFe inputs estimated here from glacial sources are noteworthy in comparison (~1–15% of Fe demand for low-chlorophyll years, 0.5–5% in high-chlorophyll years). As discussed above, this likely significantly underestimates total glacial input, including basal ice and runoff. As an example, if basal ice and glacial runoff each made a 1% contribution to the meteoric water inventory (likely conservative given the exposed rock surrounding Ryder Bay), the glacial Fe supply would account for 3–70% of Fe demand for a low-chlorophyll year, and 2–22% for a high-chlorophyll year. Whilst speculative regarding the potential contributions of basal ice and runoff to glacial Fe supply, this analysis highlights that glacial inputs are a substantial source of Fe to an area which is unlikely to be Fe-deficient due to the ratios of vertical nutrient fluxes. As such, there is an excess supply of Fe from glacial inputs to Ryder Bay.

5. Conclusions and implications

Using time series measurements of dFe and TDFe throughout a bloom, we identify sources of Fe and their relative contributions to seasonal Fe cycling at a coastal southern WAP station. This has allowed us to budget upward nutrient fluxes, and combined with the seasonal dFe minimum indicates that Fe does not limit primary production in Ryder Bay.

This study identifies sedimentary input (deep water) as a key Fe source that is greater than glacial sources over annual or longer timescales. Ratios of macronutrients versus Fe concentrations in deep waters indicate that macronutrients will be depleted before Fe becomes limiting. Thus, Fe will not be fully utilised in the WAP region, and has the potential to be transported to offshore, Fe-limited areas.

On shorter timescales, this study also identifies significant glacial Fe inputs; in contrast, Fe inputs from sea-ice appear minor. Glacial sources are active during the growing period, especially early in the summer, and the magnitude of this seasonal supply (up to 1.9–19.5 μmol Fe m^{-2}, , not including any basal ice or runoff) is significant with respect to the estimated biological Fe demand (130–400 μmol Fe m^{-2}). Some of this Fe may be rapidly recycled via the biota, and all indices measured here suggest an Fe-replete phytoplankton community, well above any threshold for Fe stress.

The WAP is currently an Fe source region (de Baar et al., 1995; Holeton et al., 2005; de Jong et al., 2012; Hatta et al., 2013), and continued warming is likely to affect the magnitude of this source. Stronger and/or more frequent CDW incursions as changes in atmospheric circulation in the region proceed (Martinson et al., 2008; Meredith et al., 2010) may supply Fe to WAP waters by increasing the amount of water flowing over the shelf in direct contact with sediments. Ongoing glacial melt and retreat (Vaughan, 2006; Rignot et al., 2014) will increase Fe input, and retreat of marine terminating glaciers could expose additional subglacial sediments, enhancing seawater driven sediment mixing and Fe release. This Fe has the potential to be transported off the WAP shelf, as it can be advected to some extent into the ACC (Hofmann et al., 1996; Zhou et al., 2002; Beardsley et al., 2004; Klinck et al., 2004). In particular, offshore transport of particulate glacial Fe may represent a significant flux of Fe to the Southern Ocean, consistent with the WAP region being a source of Fe to the ACC (de Jong et al., 2012). This represents a pathway delivering Fe to offshore regions that are currently Fe-limited, where it could stimulate primary production and promote C drawdown, acting as a negative-feedback mechanism on atmospheric CO_2.

Acknowledgements

The authors would like to thank the marine staff of Rothera Research Station for help with sample collection, and the British Antarctic Survey for logistical support. Antarctic fieldwork work was supported through the Collaborative Gearing Scheme of the British Antarctic Survey (through NERC, UK, CGS11/56). Scholarship funding was provided to A.L.A. by the School of GeoSciences (University of Edinburgh), and NSERC (Canada), PGSD-374281-2009. We are grateful to the Associate Editor and two anonymous reviewers for comments which have greatly improved the manuscript. RaTS data can be requested at www.antarctica.ac.uk/rats, other data are available from the authors.

References

Annett, A.L., 2013. Phytoplankton Ecology and Biogeochemistry of the Warming Antarctic Sea-ice Zone. University of Edinburgh, Edinburgh.

Annett, A.L., Carson, D.S., Crosta, X., Clarke, A., Ganeshram, R.S., 2010. Seasonal progression of diatom assemblages in surface waters of Ryder Bay, Antarctica. Polar Biol. 33, 13–29. http://dx.doi.org/10.1007/s00300-009-0681-7.

Annett, A.L., Henley, S.F., van Beek, P., Souhaut, M., Ganeshram, R.S., Venables, H.J., Meredith, M.P., Geibert, W., 2013. Use of radium isotopes to estimate mixing rates and trace sediment inputs to surface waters in northern Marguerite Bay (Antarctic Peninsula). Antarct. Sci. 25, 445–456.

Ardelan, M.V., Holm-Hansen, O., Hewes, C.D., Reiss, C.S., Silva, N.S., Dulaiova, H., Steinnes, E., Sakshaug, E., 2010. Natural iron enrichment around the Antarctic Peninsula in the Southern Ocean. Biogeosciences 7, 11–25.

Baker, A.R., Jickells, T.D., Witt, M., Linge, K.L., 2006. Trends in the solubility of iron, aluminium, manganese and phosphorus in aerosol collected over the Atlantic Ocean. Mar. Chem. 98, 43–58.

Beardsley, R.C., Limeburner, R., Owens, W.B., 2004. Drifter measurements of surface currents near Marguerite Bay on the western Antarctic Peninsula shelf during austral summer and fall, 2001 and 2002. Deep-Sea Res. II 51, 1947–1964. http://dx.doi.org/10.1016/j.dsr2.2004.07.031.

Boyd, P.W., Jickells, T., Law, C.S., Blain, S., Boyle, E.A., Buesseler, K.O., Coale, K.H., et al., 2007. Mesoscale iron enrichment experiments 1993–2005: synthesis and future directions. Science 315, 612–617. http://dx.doi.org/10.1126/science.1131669.

Boyd, P.W., Arrigo, K.R., Strzepek, R., van Dijken, G.L., 2012. Mapping phytoplankton iron utilization: insights into Southern Ocean supply mechanisms. J. Geophys. Res. 117, 1–18. http://dx.doi.org/10.1029/2011JC007726.

Bucciarelli, E., Blain, S., Tréguer, P., 2001. Iron and manganese in the wake of the Kerguelen Islands (Southern Ocean). Mar. Chem. 73, 21–36.

Carillo, C.J., Smith, R.C., Karl, D.M., 2004. Processes regulating oxygen and carbon dioxide in surface waters west of the Antarctic Peninsula. Mar. Chem. 84 (3–4), 161–179.

Clarke, A., Meredith, M.P., Wallace, M.I., Brandon, M.A., Thomas, D.N., 2008. Seasonal and interannual variability in temperature, chlorophyll and macronutrients in northern Marguerite Bay, Antarctica. Deep-Sea Res. II 55, 1988–2006. http://dx.doi.org/10.1016/j.dsr2.2008.04.035.

Cook, A.J., Fox, A.J., Vaughan, D.G., Ferrigno, J.G., 2005. Retreating glacier fronts on the Antarctic Peninsula over the past half-century. Science 308, 541–544. http://dx.doi.org/10.1126/science.1109164.

Cutter, G., Andersson, P., Codispoti, L., Croot, P., Francois, R., Lohan, M., Obata, H., Rutgers van der Loeff, M., 2010. Sampling and sample-handling protocols for GEOTRACES cruises. http://www.geotraces.org/images/stories/documents/intercalibration/Cookbook.pdf.

de Baar, H.J.W., de Jong, J.T.M., 2001. Distributions, sources and sinks of iron in seawater. In: Turner, D., Hunter, K. (Eds.), The Biogeochemistry of Iron in Seawater. John Wiley & Sons Ltd., Chichester, pp. 123–253.

de Baar, H.J.W., de Jong, J.T.M., Bakker, D.C.E., Loscher, B.M., Veth, C., Bathmann, U., Smetacek, V., 1995. Importance of iron for plankton blooms and carbon dioxide drawdown in the Southern Ocean. Nature 373, 412–415.

de Jong, J., Schoemann, V., Lannuzel, D., Croot, P., de Baar, H., Tison, J.-L., 2012. Natural iron fertilization of the Atlantic sector of the Southern Ocean by continental shelf sources of the Antarctic Peninsula. J. Geophys. Res. 117, 1–25. http://dx.doi.org/10.1029/2011JG001679.

Dulaiova, H., Ardelan, M.V., Henderson, P.B., Charette, M.A., 2009. Shelf-derived iron inputs drive biological productivity in the southern Drake Passage. Glob. Biogeochem. Cycles 23. http://dx.doi.org/10.1029/2008GB003406.

Frew, R.D., Hutchins, D.A., Nodder, S., Sanudo-Wilhelmy, S., Tovar-Sanchez, A., Leblanc, K., Hare, C.E., Boyd, P.W., 2006. Particulate iron dynamics during Fe cycle in subantarctic waters southeast of New Zealand. Glob. Biogeochem. Cycles 20.

Froelich, P.N., Klinkhammer, G.P., Bender, M.L., Luedtke, N.A., Heath, G.R., Cullen, D., Dauphin, P., Hammond, D., Hartman, B., Maynard, V., 1979. Early oxidation of organic matter in pelagic sediments of the eastern equatorial Atlantic: suboxic diagenesis. Geochim. Cosmochim. Acta 43, 1075–1090.

Gerringa, L.J.A., Alderkamp, A.-C., Laan, P., Thuróczy, C.-E., de Baar, H.J.W., Mills, M.M., van Dijken, G.L., van Haren, H., Arrigo, K.R., 2012. Iron from melting glaciers fuels the phytoplankton blooms in Amundsen Sea (Southern Ocean): iron biogeochemistry. Deep-Sea Res. II 71–76, 16–31. http://dx.doi.org/10.1016/j.dsr2.2012.03.007.

Green, W.J., Stage, B.R., Preston, A., Wagers, S., Shacat, J., Newell, S., 2005. Geochemical processes in the Onyx River, Wright Valley, Antarctica: major ions, nutrients and trace metals. Geochim. Cosmochim. Acta 69, 839–850.

Hatta, M., Measures, C.I., Selph, K.E., Zhou, M., Hiscock, W.T., 2013. Iron fluxes from the shelf regions near the South Shetland Islands in the Drake Passage during the austral-winter 2006. Deep-Sea Res. II 90, 89–101. http://dx.doi.org/10.1016/j.dsr2.2012.11.003.

Hawkings, J.R., Wadham, J.L., Tranter, M., Raiswell, R., Benning, L.G., Statham, P.J., Tedstone, A., Nienow, P., Lee, K., Telling, J., 2014. Ice sheets as a significant source of highly reactive nanoparticulate iron to the oceans. Nat. Commun. 5, 3929. http://dx.doi.org/10.1038/ncomms4929.

Hendry, K.R., Meredith, M.P., Measures, C.I., Rickaby, R.E.M., 2010. The role of sea ice formation in cycling of aluminium in northern Marguerite Bay, Antarctica, Est. Coast. Shelf Sci. 87, 103–112.

Henley, S.F., 2012. Climate-induced Changes in Carbon and Nitrogen Cycling in the Rapidly Warming Antarctic Coastal Ocean. University of Edinburgh, Edinburgh.

Hewes, C.D., Reiss, C.S., Kahru, M., Mitchell, B.G., Holm-Hansen, O., 2008. Control of phytoplankton biomass by dilution and mixed layer depth in the western Weddell-Scotia Confluence. Mar. Ecol. Prog. Ser. 366, 15–29. http://dx.doi.org/10.3354/meps07515.

Hofmann, E.E., Klinck, J.M., Lascara, C.M., Smith, D.A., 1996. Water mass distribution and circulation west of the Antarctic Peninsula and including Bransfield Strait. In: Ross, R.M. (Ed.), Foundations for Ecological Research West of the Antarctic Peninsula. American Geophysical Union, pp. 61–80.

Holeton, C.L., Nedelec, F., Sanders, R., Brown, L., Moore, C.M., Stevens, D.P., Heywood, K.J., Statham, P.J., Lucas, C.H., 2005. Physiological state of phytoplankton communities in the Southwest Atlantic sector of the Southern Ocean, as measured by fast repetition rate fluorometry. Polar Biol. 29, 44–52. http://dx.doi.org/10.1007/s00300-005-0028-y.

Homoky, W.B., Hembry, D.J., Hepburn, L.E., Mills, R.A., Statham, P.J., Fones, G.R., Palmer, M.R., 2011. Iron and manganese diagenesis in deep sea volcanogenic sediments and the origins of pore water colloids. Geochim. Cosmochim. Acta 75, 5032–5048. http://dx.doi.org/10.1016/j.gca.2011.06.019.

Homoky, W.B., Severmann, S., McManus, J., Berelson, W.M., Riedel, T.E., Statham, P.J., Mills, R.A., 2012. Dissolved oxygen and suspended particles regulate the benthic flux of iron from continental margins. Mar. Chem. 134–135, 59–70. http://dx.doi.org/10.1016/j.marchem.2012.03.003.

Hutchins, D.A., DiTullio, G.R., Zhang, Y., Bruland, K.W., 1998. An iron limitation mosaic in the California upwelling regime. Limnol. Oceanogr. 43 (6), 1037–1054.

Hydes, D.J., Liss, P.S., 1976. Fluorimetric method for the determination of low concentrations if dissolved aluminium in natural waters. Analyst 101, 922–931. http://dx.doi.org/10.1039/an9760100922.

Johnson, K.S., Gordon, M.F., Coale, K.H., 1997. What controls dissolved iron concentrations in the world ocean? Mar. Chem. 57, 137–161.

King, J.C., 1994. Recent climate variability in the vicinity of the Antarctic Peninsula. J. Climatol. 14, 357–369.

Klinck, J.M., 1998. Heat and salt changes on the continental shelf west of the Antarctic Peninsula between January 1994 and January 1994. J. Geophys. Res. 103, 7617–7636.

Klinck, J.M., Hofmann, E.E., Beardsley, R.C., Salihoglu, B., Howard, S., 2004. Water-mass properties and circulation on the west Antarctic Peninsula Continental Shelf in austral fall and winter 2001. Deep-Sea Res. II 51, 1925–1946. http://dx.doi.org/10.1016/j.dsr2.2004.08.001.

Lam, P.J., Bishop, J.K.B., Henning, C.C., Marcus, M.A., Waychunas, G.A., Fung, I.Y., 2006. Wintertime phytoplankton bloom in the subarctic Pacific supported by continental margin iron. Glob. Biogeochem. Cycles 20. http://dx.doi.org/10.1029/2005GB002557.

Lannuzel, D., Bowie, A.R., van der Merwe, P.C., Townsend, A.T., Schoemann, V., 2011. Distribution of dissolved and particulate metals in Antarctic sea ice. Mar. Chem. 124, 134–146. http://dx.doi.org/10.1016/j.marchem.2011.01.004.

Lohan, M.C., Bruland, K.W., 2008. Elevated Fe(II) and dissolved Fe in hypoxic shelf waters off Oregon and Washington: an enhanced source of iron to coastal upwelling regimes. Environ. Sci. Technol. 42, 6462–6468.

Lohan, M.C., Statham, P.J., Peck, L., 2008. Trace metals in the Antarctic soft-shelled clam *Laternulla elliptica*: implications for metal pollution from Antarctic research stations. Polar Biol. 24, 808–817. http://dx.doi.org/10.1007/s003000100279.

Löscher, B.M., de Baar, H.J.W., de Jong, J.T.M., Veth, C., Dehairs, F., 1997. The distribution of Fe in the Antarctic Circumpolar Current. Deep-Sea Res. II 44, 143–187.

Maldonado, M.T., Price, N.M., 1996. Influence of N substrate on Fe requirements of marine centric diatoms. Mar. Ecol. Prog. Ser. 141, 161–172.

Martin, J.H., Gordon, R.M., Fitzwater, S.E., 1990. Iron in Antarctic waters. Nature 345, 156–158.

Martinson, D.G., Stammerjohn, S.E., Iannuzzi, R.A., Smith, R.C., Vernet, M., 2008. Western Antarctic Peninsula physical oceanography and spatio-temporal variability. Deep-Sea Res. II 55, 1964–1987. http://dx.doi.org/10.1016/j.dsr2.2008.04.038.

Measures, C.I., Yuan, J., Resing, J.A., 1995. Determination of iron in seawater by flow injection analysis using in-line preconcentration and spectrophotometric detection. Mar. Chem. 50, 3–12.

Meredith, M.P., Renfrew, I.A., Clarke, A., King, J.C., Brandon, M.A., 2004. Impact of the 1997/98 ENSO on upper ocean characteristics in Marguerite Bay, western Antarctic Peninsula. J. Geophys. Res. 109. http://dx.doi.org/10.1029/2003JC001784.

Meredith, M.P., King, J.C., 2005. Rapid climate change in the ocean west of the Antarctic Peninsula during the second half of the 20th century. Geophys. Res. Lett. 32, L19604. http://dx.doi.org/10.1029/2005GL024042.

Meredith, M.P., Brandon, M.A., Wallace, M.I., Clarke, A., Leng, M.J., Renfrew, I.A., van Lipzig, N.P.M., King, J.C., 2008. Variability in the freshwater balance of northern Marguerite Bay, Antarctic Peninsula: results from $\delta^{18}O$. Deep-Sea Res. II 55, 309–322. http://dx.doi.org/10.1016/j.dsr2.2007.11.005.

Meredith, M.P., Wallace, M.I., Stammerjohn, S.E., Renfrew, I.A., Clarke, A., Venables, H.J., Shoosmith, D.R., Souster, T., Leng, M.J., 2010. Changes in the freshwater composition of the upper ocean west of the Antarctic Peninsula during the first decade of the 21st century. Prog. Oceanogr. 87, 127–143. http://dx.doi.org/10.1016/j.pocean.2010.09.019.

Meredith, M.P., Venables, H.J., Clarke, A., Ducklow, H., Erikson, M., Leng, M.J., Lenaerts, J.T.M., van den Broeke, M.R., 2013. The freshwater system west of the Antarctic Peninsula: spatial and temporal changes. J. Clim. 26, 1669–1684.

Mikucki, J.A., Pearson, A., Johnston, D.T., Turchyn, A.V., Farquhar, J., Schrag, D.P., Anbar, A.D., Priscu, J.C., Lee, P.A., 2009. A contemporary microbially maintained subglacial ferrous "ocean". Science 324, 397–400.

Moffat, C., Beardsley, R.C., Owens, B., van Lipzig, N., 2008. A first description of the Antarctic Peninsula coastal current. Deep-Sea Res. II 55, 277–293. http://dx.doi.org/10.1016/j.dsr2.2007.10.003.

Moffat, C., Owens, B., Beardsley, R.C., 2009. On the characteristics of Circumpolar Deep Water intrusions to the west Antarctic Peninsula Continental Shelf. J. Geophys. Res. 114. http://dx.doi.org/10.1029/2008JC004955.

Planquette, H., Statham, P.J., Fones, G.R., Charette, M.A., Moore, C.M., Salter, I., Nédélec, F.H., Taylor, S.L., French, M., Baker, A.R., Mahowald, N., Jickells, T.D., 2007. Dissolved iron in the vicinity of the Crozet Islands, Southern Ocean. Deep-Sea Res. II 54, 1999–2019.

Planquette, H., Fones, G.R., Statham, P.J., Morris, P.J., 2009. Origin of iron and aluminium in large particles (>53 μm) in the Crozet region, Southern Ocean. Mar. Chem. 115, 31–42. http://dx.doi.org/10.1016/j.marchem.2009.06.002.

Planquette, H., Sanders, R.R., Statham, P.J., Morris, P.J., Fones, G.R., 2011. Fluxes of particulate iron from the upper ocean around the Crozet Islands: a naturally iron-fertilized environment in the Southern Ocean. Glob. Biogeochem. Cycles 25, 1–12. http://dx.doi.org/10.1029/2010GB003789.

Planquette, H., Sherrell, R.M., Stammerjohn, S., Field, M.P., 2013. Particulate iron delivery to the water column of the Amundsen Sea, Antarctica. Mar. Chem. 153, 15–30.

Queroue, R., Sarthou, G., Planquette, H.F., Bucciarelli, E., Chever, F., van der Merwe, P., Lannuzel, D., Townsend, A.T., Cheize, M., Blain, S., d'Ovidio, F., Bowie, A.R., 2015. High variability of dissolved iron concentrations in the vicinity of Kerguelen Island (Southern Ocean). Biogeosci. Discuss. 12, 231–270. http://dx.doi.org/10.5194/bgd-12-231-2015.

Raiswell, R., 2011. Iceberg-hosted nanoparticulate Fe in the Southern Ocean. Mineralogy, origin, dissolution kinetics and source of bioavailable Fe. Deep-Sea Res. II 58, 1364–1375. http://dx.doi.org/10.1016/j.dsr2.2010.11.011.

Raiswell, R., Tranter, M., Benning, L.G., Siegert, M., De'ath, R., Huybrechts, P., Payne, T., 2006. Contributions from glacially derived sediment to the global iron (oxyhydr)oxide cycle: implications for iron delivery to the oceans. Geochim. Cosmochim. Acta 70, 2765–2780. http://dx.doi.org/10.1016/j.gca.2005.12.027.

Raiswell, R., Benning, L.G., Tranter, M., Tulaczyk, S., 2008. Bioavailable iron in the Southern Ocean: the significance of the iceberg conveyor belt. Geochem. Trans. 9. http://dx.doi.org/10.1186/1467-4866-9-7.

Rignot, E., Mouginot, J., Morlighem, M., Seroussi, H., Scheuchi, B., 2014. Widespread, rapid grounding line retreat of Pine Island, Thwaites, Smith, and Kohler glaciers, West Antarctica, from 1992 to 2011. Geophys. Res. Lett. 41, 3502–3509. http://dx.doi.org/10.1002/2014GL060140.

Sañudo-Wilhelmy, S.A., Olsen, K.A., Scelfo, J.M., Foster, T.D., Flegal, A.R., 2002. Trace metal distributions off the Antarctic Peninsula in the Weddell Sea. Mar. Chem. 77, 157–170.

Sedwick, P.N., Edwards, P.R., Mackey, D.J., Griffiths, F.B., Parslow, J.S., 1997. Iron and manganese in surface waters of the Australian subantarctic region. Deep-Sea Res. I 44, 1239–1253.

Shaw, T.J., Raiswell, R., Hexel, C.R., Vu, H.P., Moore, W.S., Dudgeon, R., Smith, K.L., 2011. Input, composition, and potential impact of terrigenous material from free-drifting icebergs in the Weddell Sea. Deep-Sea Res. II 58, 1376–1383. http://dx.doi.org/10.1016/j.dsr2.2010.11.012.

Sheppard, D.S., Deely, J.M., Edgerley, W.H.L., 1997. Heavy metal content of meltwaters from the Ross Sea Dependency, Antarctica. N. Z. J. Mar. Freshw. Res. 31, 313–325. http://dx.doi.org/10.1080/00288330.1997.9516769.

Stammerjohn, S.E., Martinson, D.G., Smith, R.C., Iannuzzi, R.A., 2008. Sea ice in the western Antarctic Peninsula region: spatio-temporal variability from ecological and climate change perspectives. Deep-Sea Res. II 55, 2041–2058. http://dx.doi.org/10.1016/j.dsr2.2008.04.026.

Statham, P.J., Skidmore, M., Tranter, M., 2008. Inputs of glacially derived dissolved and colloidal iron to the coastal ocean and implications for primary productivity. Glob. Biogeochem. Cycles 22. http://dx.doi.org/10.1029/2007GB003106.

Sunda, W.G., Huntsman, S.A., 1995. Iron uptake and growth limitation in oceanic and coastal phytoplankton. Mar. Chem. 50, 189–206.

Tappin, A.D., Millward, G.E., Statham, P.J., Burton, J.D., Morris, A.W., 1995. Trace-metals in the central and southern North Sea. Estuar. Coast. Shelf Sci. 41, 275–323.

Thuroczy, C.-E., Alderkamp, A.-C., Laan, P., Gerringa, L.J.A., Mills, M.M., Van Dijken, G.L., De Baar, H.J.W., Arrigo, K.R., 2012. Key role of organic complexation of ion in sustaining phytoplankton blooms in the Pine Island and Amundsen Polynyas (Southern Ocean). Deep-Sea Res. II 71–76, 49–60.

Twining, B.S., Baines, S.B., 2013. The trace metal composition of marine phytoplankton. Ann. Rev. Mar. Sci. 5, 191–215. http://dx.doi.org/10.1146/annurev-marine-121211-172322.

Twining, B.S., Baines, S.B., Fisher, N.S., Landry, M.R., 2004. Cellular iron contents of plankton during the Southern Ocean Iron Experiment (SOFeX). Deep-Sea Res. I 51, 1827–1850. http://dx.doi.org/10.1016/j.dsr.2004.08.007.

Twining, B.S., Nodder, S.D., King, A.L., Hutchins, D.A., LeCleir, G.R., DeBruyn, J.M., Maas, E.W., Vogt, S., Wilhelm, S.W., Boyd, P.W., 2014. Differential remineralization of major and trace elements in sinking diatoms. Limnol. Oceanogr. 59, 689–704. http://dx.doi.org/10.4319/lo.2014.59.3.0689.

Vaughan, D.G., 2006. Recent trends in melting conditions on the Antarctic Peninsula and their implications for ice-sheet mass balance and sea level. Arct. Antarct. Alp. Res. 38, 147–152.

Vaughan, D.G., Marshall, G.J., Connolley, W.M., Parkinson, C., Mulvaney, R., Hodgson, D.A., King, J.C., Pudsey, C.J., Turner, J., 2003. Recent rapid regional climate warming on the Antarctic Peninsula. Clim. Chang. 60, 243–274.

Venables, H.J., Clarke, A., Meredith, M.P., 2013. Wintertime controls on summer stratification and productivity at the western Antarctic Peninsula. Limnol. Oceanogr. 58 (3), 1035–1047.

Wagener, T., Guieu, C., Losno, R., Bonnet, S., Mahowald, N., 2008. Revisiting atmospheric dust export to the Southern Hemisphere ocean: biogeochemical implications. Glob. Biogeochem. Cycles 22. http://dx.doi.org/10.1029/2007GB002984.

Wallace, M.I., Meredith, M.P., Brandon, M.A., Sherwin, T.J., Dale, A., Clarke, A., 2008. On the characteristics of internal tides and coastal upwelling behaviour in Marguerite Bay, west Antarctic Peninsula. Deep-Sea Res. II 55, 2023–2040. http://dx.doi.org/10.1016/j.dsr2.2008.04.033.

Wedepohl, K., 1995. The composition of the continental crust. Geochim. Cosmochim. Acta 59, 1217–1232.

Westerlund, S., Öhman, P., 1991. Iron in the water column of the Weddell Sea. Mar. Chem. 35, 199–217. http://dx.doi.org/10.1016/S0304-4203(09)90018-4.

Weston, K., Jickells, T.D., Carson, D.S., Clarke, A., Meredith, M.P., Brandon, M.A., Wallace, M.I., Ussher, S.J., Hendry, K.R., 2013. Primary production export flux in Marguerite Bay (Antarctic Peninsula): linking upper water-column production to sediment trap flux. Deep-Sea Res. I 75, 52–66.

Wu, J., Luther III, G.W., 1996. Spatial and temporal distribution of iron in the surface water of the northwestern Atlantic Ocean. Geochim. Cosmochim. Acta 60, 2729–2741.

Zhou, M., Niiler, P.P., Hu, J.-H., 2002. Surface currents in the Bransfield and Gerlache Straits, Antarctica. Deep-Sea Res. I 49, 267–280.